Chemical Engineering Journal 158 (2010) 418–425

Contents lists available at ScienceDirect

Chemical Engineering Journal

journal homepage: www.elsevier.com/locate/cej

# Dual-effects of adsorption and photodegradation of methylene blue by tungsten-loaded titanium dioxide

Saepurahman, M.A. Abdullah*, F.K. Chong

*Department of Chemical Engineering, Universiti Teknologi Petronas, Bandar Seri Iskandar, 31750 Tronoh, Perak D.R., Malaysia*

ARTICLE INFO

*Article history:*
Received 3 August 2009
Received in revised form
31 December 2009
Accepted 7 January 2010

*Keywords:*
Photocatalysis
Adsorption
Titanium dioxide
Tungsten loading
Environmental remediation

ABSTRACT

Surface modification of titanium dioxide ($TiO_2$) with tungsten was carried out to increase the photocatalytic degradation of methylene blue (MB). The modified photocatalyst in dark experiment had high affinity towards MB with the amount adsorbed proportional to the tungsten loading and the highest adsorption was at 6.5 mol% tungsten loading. The adsorption isotherm study showed that the adsorption followed Langmuir model with maximum adsorption capacity of $95.9 \times 10^{-3}$ mmol $g^{-1}$, 8-fold higher than the reported value for unmodified $TiO_2$. Under illumination, the modified photocatalyst also enhanced the degradation of MB as compared to the unmodified one. Kinetic studies on the photocatalytic degradation of MB using linear and non-linear regression methods suggested that the degradation followed first order kinetics. The photocatalytic activity was greatly affected by the amount of tungsten loading, calcination temperature and calcination duration. The optimum synthesis condition was found at 1 mol% tungsten loading and calcination at 450 °C for 2 h. Using UV filter, the DRUV-Vis analysis confirmed that the enhancement of the photocatalytic activity was not due to the extension of the photoresponse into the visible region. The presence of UV portion rather enhanced the photocatalytic activity.



## 1. Introduction

Photocatalysis is a catalytic reaction under the action of light in the presence of a photocatalyst [1]. $TiO_2$ photocatalysis is attractive due to the possibility of utilizing solar source as a renewable energy. In addition, $TiO_2$ is inexpensive where titanium is the world's seventh most abundant metal and ninth most abundant element [2,3]. $TiO_2$ is non-toxic and has found applications as white pigment and UV absorber in food and paint industries and in cosmetics preparations [3]. $TiO_2$ is chemically and photo-chemically stable, resistant to corrosion and photo-corrosion, and can be activated by UV light shorter than 388 nm [3–5]. The major drawback in $TiO_2$ photocatalysis though is its lack of efficiency due to the high rate of recombination of electrons and holes upon photoactivation [5]. Due to its wide bandgap energy, $E_g$, of 3.0–3.2 eV, it can only be activated by UV light, which coincidentally accounts only 3–4% of sunlight spectrum [6]. Although many semiconductors such as CoO, $Fe_2O_3$, MnO, $V_2O_5$ and $WO_3$ have wide bandgap energy ($E_g$ 2.0–3.6 eV) and are inefficient as photocatalysts, $E_g$ may not be the only factor governing the photocatalytic activity. Other important factors for effective photocatalysis are particle sizes, surface properties, and phase compositions. Efforts have been made to enhance the efficiency of the process and to modify electronic properties of $TiO_2$ so that it can utilize higher portion of solar spectrum. $TiO_2$ has been modified with different group of metals such as alkaline metals [7], earth alkaline metals [8,9], transition metals [10–13], rare earth metals [14,15], and noble metals [16]. Among transition metal dopant, cobalt and tungsten are reportedly the best for photodegradation of 4-nitrophenol, benzoic and methanoic acid, while samarium is best for 2-propanol degradation [13,17–19].

Dyes, representing some 9000 colouring agents of which 70% are azo dyes [20], have been of environmental concern due to indiscriminate discharge by textile industries. Discharged dyes do not only affect the water quality, but also affect health as some of these are mutagenic, carcinogenic and teratogenic. Dyes such as benzidine, 2-naphtyl amine and its derivatives are known as human bladder carcinogens and are subjected to water regulation and policy [21]. Physical adsorption of discharged dyes by activated carbon is an economically effective process, while adsorption by other adsorbents such as bagasse, woodchips, and peat is gaining attention due to its abundance as agricultural by-products that require no activation. However, all these processes may merely transfer the waste materials from the effluent to the adsorbent. There is a need for post-treatment such as incineration of the wastes adsorbed. Biological methods (aerobic and anaerobic processes) and chemical methods (Fenton's reagent, ozonation, sodium hypochlorite oxidation, and electrochemical oxidation) involve the transformation of the pollutant into a product that does not absorb wavelength in the visible region of the spectrum. Photocatalysis has several

* Corresponding author. Tel.: +60 5 3687636; fax: +60 5 3656176.
*E-mail address:* azmuddin@petronas.com.my (M.A. Abdullah).

1385-8947/$ – see front matter © 2010 Elsevier B.V. All rights reserved.
doi:10.1016/j.cej.2010.01.010

advantages as it uses no reagent and the degradation of dyes occurs at ambient pressure and temperature.

Adsorption of a pollutant onto adsorbent is affected by temperature of the process [22]. Adsorption isotherm study allows the quantification of the maximum amount of pollutant adsorbed per mass of adsorbent at definite temperature. Modelling of the adsorption data allows better understanding on the mechanism of the adsorption process. Different adsorption models have been proposed such as Langmuir, Freundlich and Redlich-Peterson [23]. Kinetic analysis further allows the quantification of the photocatalytic process and comparison of the effects of different synthesis parameters such as effect of initial concentration, photocatalyst loading, initial pH, tungsten loading and calcination temperature and time length [3]. Adsorption of a compound onto photocatalyst surface is one of key reaction steps in photocatalysis. However, due to its hydrophilic nature, $TiO_2$ exhibits low adsorption ability especially to non-polar compounds [24]. To improve the adsorption ability, $TiO_2$ has been loaded onto various adsorbent such as MCM-41, beta zeolite, montmorillonite, and synthetic 13-x, Na-Y, and 4A-zeolites [24,25]. $TiO_2$-adsorbent system offers good adsorption towards pollutant and easier separation. $TiO_2$ loaded onto natural zeolite (mordenite) is active for the degradation of methyl orange [26]. Loading of noble metals such platinum [27] and yttrium [28] onto $TiO_2$–zeolite system give further enhancement in the photocatalytic activity. Some have shown better photocatalytic activity in orange II dye degradation than the commercial Degussa P25 [24]. To our knowledge, degradation of MB by tungsten-loaded $TiO_2$ has not been reported in great detail.

The aim of this study was to assess the photocatalytic activity of tungsten-loaded $TiO_2$. The profile of MB removal by adsorption process, followed by photodegradation was established. The kinetics analysis and modelling of MB removal via adsorption and photodegradation were carried out. The optimization of synthetic procedure based on the effects of tungsten loading, calcination temperature and time length on the kinetics of photodegradation were also studied.

## 2. Materials and methods

### 2.1. Preparation

$TiO_2$ Degussa P25 (Degussa, Germany) was weighed and dispersed in distilled water and an appropriate amount of aqueous solution of ammonium metatungstate (AMT) solution was added. The suspension was stirred overnight to equilibrate the adsorption–desorption processes. The suspension was evaporated to dryness using a waterbath, and further dried in an oven at 120 °C overnight. The powder was then ground using mortar and pestle and then calcined at different temperatures and duration using a programmable furnace (Nabertherm, Germany) with ramp rate at 3.5 °C/min under static air. The powder was subsequently sieved prior to characterization or decolourization studies. The photocatalyst was denoted based on tungsten loading, calcination temperature and calcinations duration. Unless otherwise stated, all experiments were carried out using 1-w-450-2 photocatalyst which represents 1 mol% $WO_3$ loading and calcination at 450 °C for 2 h.

### 2.2. Decolourization studies

To establish the dual-effects of adsorption-photodegradation of MB on tungsten-loaded $TiO_2$ photocatalyst, sample was weighed and mixed with 10 mL of distilled water in a glass dish. The suspension was ultrasonicated for 10 min using ultrasonicator (Barnstead, USA), followed by addition of MB solution to give a concentration of 40 ppm in 100 mL and catalyst loading of 1 g/L. The dish was covered with a glass closure and left to ambient temperature of 26–29 °C. Initial pH of the solution was 6. The suspension was kept in the dark condition and continuously stirred using a magnetic stirrer (Ika, Germany) to equilibrate the adsorption–desorption processes. After 4 h, the dish was illuminated with a 250 W metal halide lamp (Venture Lighting, USA) of 21,000 lx intensity, at a distance of 5 cm from the top of the glass closure. The spectral distribution of the lamp is between 380 and 760 nm with peak of emission at 590 nm.

Adsorption isotherm studies were carried out to determine the adsorption characteristics of the photocatalyst. Experiments were conducted using a double jacketed reactor where the temperature was maintained at 25 °C using a circulated waterbath (Grant, UK). The reactor was wrapped with aluminium foil to prevent the any incident light from external sources. Sample photocatalyst was weighed and mixed with distilled water and then ultrasonicated for 10 min using an ultrasonicator (Barnstead, USA). Then, it was mixed with MB solution at different concentration to give catalyst concentration of 1 g/L and in a total volume of 100 mL volume. The suspension was mechanically stirred using an impeller (Heidolph, Germany). Five hundred microliter of the suspension was taken at fixed intervals where it was centrifuged two times at $2000 \times g$ (Sigma, USA) to remove any particulate. The concentrations of MB in the sample were determined using Shimadzu 3150 UV–Vis Spectrometer, Japan, at $\lambda = 664.50$ nm.

### 2.3. Kinetics and modeling

Photocatalytic degradation of MB yields carbon dioxide, nitrate, sulfate and water. The reaction can be written as follows [29]:

$$C_{16}H_{18}N_3S^+ + 25.5O_2 \rightarrow 16CO_2 + 3NO_3^- + SO^{2-} + 6H^+ + 6H_2O \quad (1)$$

or in a simplified form:

$$MB + \cdots O_2 \rightarrow \cdots CO_2 + \cdots \quad (2)$$

Rate of MB consumed in the reaction can be written as:

$$r = -\frac{d[MB]}{dt} = k[MB]^n \quad (3)$$

where $n$ is order of reaction. If the reaction follows zeroth and first order kinetics, integration of Eq. (3) gives Eqs. (4) and (5), respectively.

$$[MB]_e - [MB]_t = k_0 t \quad (4)$$

$$\ln\frac{[MB]_t}{[MB]_e} = -k_1 t \quad (5)$$

where $[MB]\,e$, $t$ respectively indicates MB concentration at $t = 0$ and $t = t$.

Eq. (5) can be rewritten into a non-linear form as shown in Eq. (6)

$$[MB]_t = [MB]_e e^{-k_1 t} \quad (6)$$

If the reaction follows second order kinetics, integration of Eq. (3) gives Eq. (7) which can also be rewritten in a non-linear form as shown in Eq. (8).

$$\frac{1}{[MB]_t} - \frac{1}{[MB]_e} = k_2 t \quad (7)$$

$$[MB]_t = \frac{[MB]_e}{[MB]_e k_2 t + 1} \quad (8)$$

Adsorption of pollutant onto adsorbent can be modelled by mathematical models such as Langmuir, Freundlich and Redlich-Peterson model. Amount of MB adsorbed onto photocatalyst at time

$t$ was determined using Eq. (9) [22].

$$Q = \frac{(C_0 - C_t)V_{Tot}}{[Cat]} \quad (9)$$

where $C_0$ and $C_t$ is the MB concentration (mg/L) at initial and at time $t$, while $V_{Tot}$ and $[Cat]$ are the total volume (L) and catalyst mass (g), respectively. The amount of MB adsorbed onto the photocatalyst at equilibrium is defined as $Q_e$, whereas its concentration at equilibrium is $C_e$.

The mathematical formulae of Langmuir and Freundlich models are shown in Eqs. (10) and (11), respectively. Both equations can be rewritten into linear form as shown in Eqs. (12) and (13), respectively.

$$Q_e = \frac{Q_m K_a C_e}{1 + K_a C_e} \quad (10)$$

$$Q_e = K_F C_e^{1/n} \quad (11)$$

$$\frac{C_e}{Q_e} = \frac{1}{Q_m} C_e + \frac{1}{K_a Q_m} \quad (12)$$

$$\ln(Q_e) = \ln(K_F) + \frac{1}{n}\ln(C_e) \quad (13)$$

To examine the model fitness with the experimental data, coefficient of determination ($r^2$) and sum of square error (SSE), which were generated automatically from MATLAB® using cftool toolbox, were used. The model is considered best fit when $r^2$ is close to 1, while SSE is as minimum as possible.

## 3. Results and discussion

### 3.1. Decolourization profiles of MB

Fig. 1 shows the decolourization profile of MB as a function of tungsten loadings. In the absence of light (dark experiment), the adsorption process took place. Adsorptions of MB by unmodified $TiO_2$ (0-w-450-2) and pure $WO_3$ (AMT-w-450-2) were negligible but the adsorption became more apparent with increasing tungsten loadings. The amount of MB adsorbed increased linearly, concomitant with the increase in tungsten loadings from 2 to 5 mol%. The adsorption rate was minimal for pure $WO_3$ and unmodified $TiO_2$ suggesting the need for available surface area and binding sites for MB to occupy the surface. The adsorption reached equilibrium within 10 min and no further adsorption was observed with prolonged duration. The colour of tungsten-loaded photocatalyst changed from white to dark blue at the end of dark experiment. The sharp L-shaped adsorption profiles suggest that there are no significant competitions between MB and water molecules during the adsorption process [3,30]. We have recently reported the mass titration curve of tungsten-loaded $TiO_2$ [31] and the profile was similar to the MB adsorption profile. The point-zero-charge (PZC) values decreased from 6.35 at 0-w-450-2, to around 3, with increasing tungsten loading up to 6.5 mol% $WO_3$. No appreciable changes in the PZC values were observed with further loading [31].

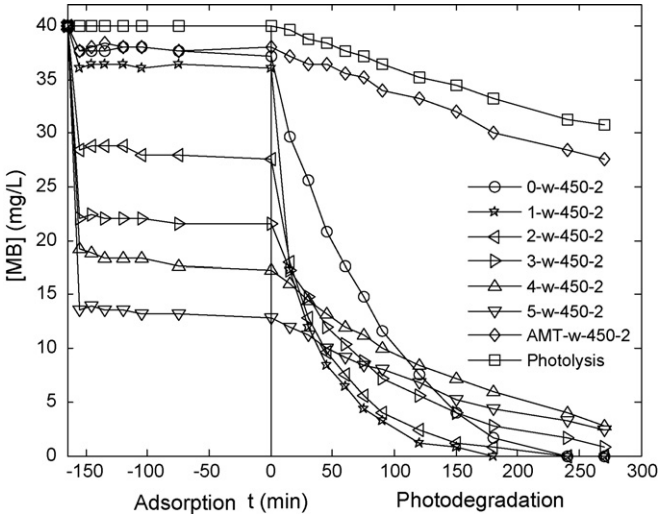


**Fig. 1.** Decolourization of MB by tungsten-loaded $TiO_2$ through adsorption and photodegradation processes.

When the light source was switched on, the photocatalytic reaction ensued. The bluish colour of MB-adsorbed photocatalyst faded slowly to purple and finally returned to its original white colour. The photodegradation of MB under light only without the photocatalyst (photolysis), or under $WO_3$ only, was negligible. The rate of MB decolourization was increasing in the order of unmodified $TiO_2$, followed by tungsten-loaded $TiO_2$, as shown by the steeper slope in Fig. 1. Higher photocatalytic activity occurred at 1–2 mol% tungsten loading, but slower at 3–5 mol% tungsten loading. Hence, higher tungsten loading (3–5 mol%) had resulted in higher adsorption capacity, but lower photocatalytic activity. There appears to be a threshold level of tungsten level beyond which the amount of incident light could have been reduced from reaching the photocatalyst. This can be attributed to the higher degree of agglomeration of photocatalyst at higher tungsten loadings [31].

Similar to our study, samarium, neodynium, and praseodymium-doped $TiO_2$ have been reported to possess higher adsorption and photocatalytic activities than the bare $TiO_2$ [32]. However, other study based on the flame-made $WO_3/TiO_2$ [28] report that MB is completely adsorbed in the dark not only for sample containing $\geq$7.2 mol% $WO_3$, but also pure $WO_3$. The study suggests that the increase in the adsorption of MB can be correlated to the increase in the acid strength [33]. W-doped $TiO_2$ prepared from the sol–gel method has maximum adsorption towards crystal violet at pH 7, with 6 mol% W achieving adsorption 10-fold higher than the bare $TiO_2$ [34]. However, when it is normalized with respect to the surface area, the adsorption capacity remains constant suggesting that the increase in the adsorption towards crystal violet is due to the increasing surface area. Hence, the improvement in the photocatalytic activity is essentially in finding the balance between having higher sorption capacity and a lower reduction in the specific activity of each adsorption site.

### 3.2. Adsorption of MB

Fig. 2 shows the adsorption of MB as a function of tungsten loadings. The MB adsorbed by unmodified $TiO_2$ and 1-w-450-2 were below 5 mg/L but increased proportionally to almost 6-fold for 6.5-w-450-2. At tungsten loading >6.5 mol% $WO_3$, the MB adsorbed was reduced which confirmed the threshold level of tungsten as discussed earlier. Akurati et al. [33] have reported complete adsorption by pure $WO_3$, but in our study the adsorption of MB by pure $WO_3$ was negligible. The difference is possibly due to the difference in particle size to that reported in the former as a result of different method of preparation.

The effect of initial MB concentration was investigated at 6.5 mol% $WO_3$ loading (Fig. 3). The value of MB adsorbed at equilibrium, $Q_e$, was used to study the adsorption isotherm behaviour. The amount of MB adsorbed increased 3-fold by increasing the initial MB concentrations from 10 to 30 mg/L. Further increase up to 45 mg/L did not significantly increase the amount of MB adsorbed. The increase in the initial MB concentration enhanced the amount of MB adsorbed until all the adsorption sites were occupied. The amount of MB adsorbed or desorbed finally became constant at equilibrium. Hence, the adsorption curves are superimposed [22] beyond 30 mg/L initial MB concentration.

**Table 1**
Adsorption isotherm modeling of MB onto 6.5-w-450-2.

| Isotherm model | Equation | Linear form | Plot | Parameters | | $r^2$ | SSE |
|---|---|---|---|---|---|---|---|
| Linear regression analysis | | | | | | | |
| Freundlich | $Q_e = K_F C_e^{1/n}$ | $\ln(Q_e) = \ln(K_F) + \frac{1}{n}\ln(C_e)$ | $\ln Q_e$ vs. $\ln C_e$ | $K_F = 20.7$ | $n = 5.2$ | 0.58 | 0.42 |
| Langmuir | $Q_e = \frac{Q_m K_a C_e}{1 + K_a C_e}$ | $\frac{C_e}{Q_e} = \frac{1}{Q_m} C_e + \frac{1}{K_a Q_m}$ | $\frac{C_e}{Q_e}$ vs. $C_e$ | $K_a = 4.1$ | $Q_m = 30.7$ | 0.99 | 0.00 |
| Non-linear regression analysis | | | | | | | |
| Freundlich | $Q_e = K_F C_e^{\frac{1}{n}}$ | – | – | $K_F = 22.1$ | $n = 7.0$ | 0.62 | 132.50 |
| Langmuir | $Q_e = \frac{Q_m K_a C_e}{1 + K_a C_e}$ | – | – | $K_a = 3.6$ | $Q_m = 31.5$ | 0.82 | 59.70 |

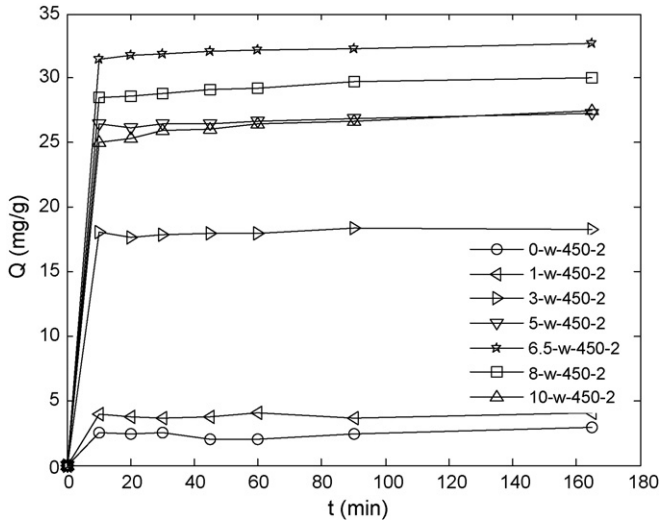


**Fig. 2.** Effect of tungsten loadings on MB adsorption.

Figs. 4 and 5 show adsorption isotherm model of MB at 6.5-w-450-2 using both non-linear and linear regression. Langmuir model provides better fitting to the adsorption data compared to the Freundlich model with coefficient of determination, $r^2 = 0.99$. Table 1 summarizes the modeling of adsorption of MB onto 6.5-w-450-2. Based on Langmuir, MB adsorption onto 6.5-w-450-2 may have formed monolayer instead of multilayer surface. The maximum adsorption capacity, $Q_m$, at 30.7 mg $g^{-1}$ was equivalent to $95.9 \times 10^{-3}$ mmol $g^{-1}$. This is approximately 8-fold higher than the reported value for unmodified $TiO_2$ at $11.7 \times 10^{-3}$ mmol $g^{-1}$ [30]. This may be attributable to the molecular size of the substrates, the compatibility of chemical charges or physisorption and the higher availability of adsorption sites. For comparison, the $Q_m$ for orange G is $9.14 \times 10^{-3}$, alizarin S $12 \times 10^{-3}$, methyl red $6.29 \times 10^{-3}$, and congo red $18.24 \times 10^{-3}$ mmol $g^{-1}$ [29]. Other than dyes, the $Q_m$ of $TiO_2$ for salicylic acid is 0.07, 4-aminobenzoic acid 0.071, 3-chloro-4-hydrobenzoic acid 0.047, dichloroethane acid 0.225, 2-chlorophenol 0.107 and phenol 0.207 mmol $g^{-1}$ [22].

In comparison to our previous work on adsorption of natural product alizarin onto microporous polymeric adsorbent, the $Q_m$ of 6.5-w-450-2 is relatively lower than XAD-16 ($Q_m = 42.2$ mg $g^{-1}$ equivalent to $176.51 \times 10^{-3}$ mmol $g^{-1}$) [23]. The higher adsorption capacity of XAD-16 can be attributed to the higher surface area at 800 $m^2/g$. The surface area of 6.5-w-450-2 is estimated to be lower than the surface area of the unmodified $TiO_2$ at 50 $m^2/g$. Considering that the ratio of the surface area of XAD-16 at approximately 16-fold higher than for 6.5-w-450-2, the adsorptivity of the latter in actual fact is relatively higher, as its $Q_m$ is only half that of XAD-16. Nevertheless as highlighted earlier, the adsorption process is governed not only by specific surface area but also by pore diameter, polarity of the adsorbent, and solubility and polarity of the adsorbate [23].

### 3.3. Photodegradation of MB

The subsequent step to adsorption of MB onto the photocatalyst, was the photodegradation of MB. For quantitative evaluation, the classical zeroth, first and second order kinetics equations were fitted to the experimental data to determine the suitable model to represent the kinetic of degradation. Fig. 6 shows an example of

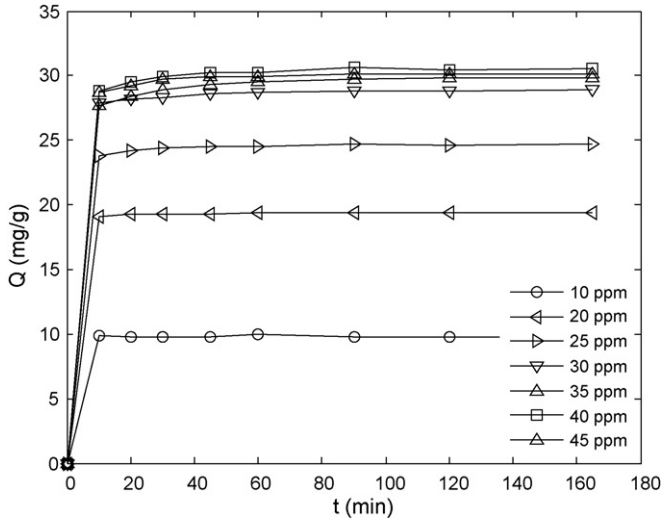


**Fig. 3.** Effect of initial concentrations on MB adsorption at 6.5-w-450-2.

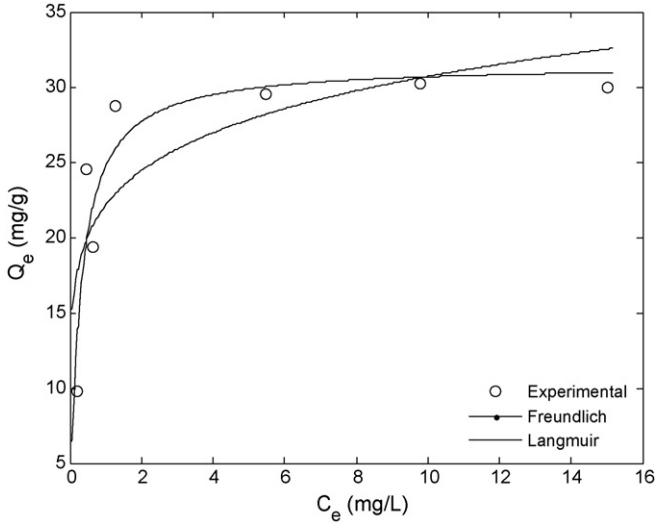


**Fig. 4.** Adsorption isotherm modeling using non-linear regression.

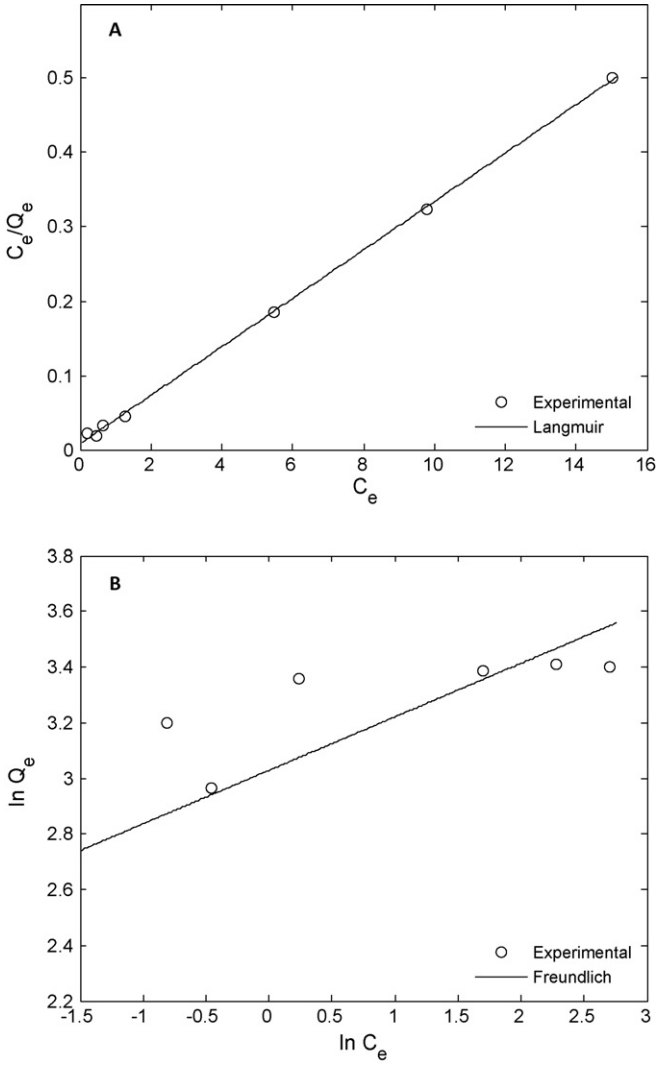


**Fig. 5.** Adsorption isotherm modeling using linear regression (A) Langmuir and (B) Freundlich.

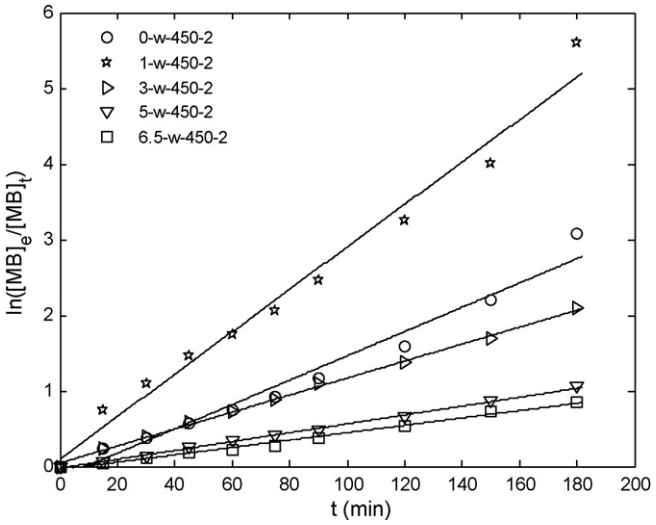


**Fig. 6.** First order kinetic modeling of MB photodegradation at different tungsten loadings.

the fitting of MB degradation to first order kinetic model. Table 2 summarizes the fitting of the photodegradation data with various kinetics models. The kinetic data of unmodified $TiO_2$ fits fairly well to zeroth order model ($r^2$ = 0.90–0.99) at higher tungsten loading but not at lower tungsten loading ($r^2$ = 0.62). Increase in tungsten loadings increases the adsorption capacity, hence the better fitting to the model. At 1 mol% tungsten loading, high degree of deviation (SSE = 403.39) was observed but with increasing tungsten loadings, SSE value decreased (SSE = 31.63–0.09). Although certain photocatalytic reactions by bare or modified $TiO_2$ follow zeroth order kinetics [35–37], our study showed that zeroth order model may not describe the kinetics well and only to a certain degree fits well for higher tungsten loadings. Based on linear and non-linear regression method, the photocatalytic degradation of MB is best represented by first order kinetic as shown in Table 2, with $r^2$ within the range of 0.97–0.99. The data however is more suitably fitted to linear regression (SSE = 0–0.48) as compared to non-linear regression (SSE = 0.36–28.25). The second order kinetic using linear method does not represent the kinetic of degradation by unmodified $TiO_2$ and $TiO_2$ loaded with 1 mol% $WO_3$ ($r^2$ = 0.70 and 0.55), though higher tungsten loadings showed better fitness ($r^2$ = 0.91–0.95). Non-linear regression gives better representation of only the first order kinetics with the coefficients of determination ranging from 0.97 to 0.98. However, all order of kinetics could describe reasonably well the MB degradation at loading greater or equal to 5 mol% using linear regression.

The degradation of pollutant may follow different kinetics depending on the method to assess the activity (disappearance of pollutant or mineralization). The degradation of oxalic acid by platinum, argentum, and aurum-modified $TiO_2$ for example follow zero order kinetic and has been reportedly doubled as compared to unmodified $TiO_2$. However, contrary to our study, the amount of oxalic acid adsorbed onto photocatalyst decreases with increasing noble metal content. Further, the photocatalytic activity is influenced by the metal size and the pH during synthesis [37]. Type of metal also affected the degradation kinetics. The decomposition of nitrite by samarium, cerium, erbium, praseodymium, lanthanum and neodymium-doped $TiO_2$ obey zero order kinetics, while the decomposition reaction using gadolinium-doped $TiO_2$ and P25 follow first order kinetics [14]. Other researchers have reported first order kinetics in the degradation of 4-nitrophenol using $WO_3/TiO_2$ [38], degradation of methylene blue using $WO_x$–$TiO_2$ [39], and

**Table 2**
Linear and non-linear regression analysis of photocatalytic kinetics of MB degradation.

| Sample | Linear regression analysis | | | | | | | | | Non-linear regression analysis | | | | | |
|---|---|---|---|---|---|---|---|---|---|---|---|---|---|---|---|
| | Zeroth order $[MB]_e - [MB]_t = k_0 t$ | | | First order $\ln[MB]_e/[MB]_t = k_1 t$ | | | Second order $1/[MB]_t - 1/[MB]_e = k_2 t$ | | | First order $[MB]_t = [MB]_e \exp(-k_1 t)$ | | | Second order $[MB]_t = [MB]_e/(k_2[MB]_e t + 1)$ | | |
| | $k_0 \times 10^{-3}$ | $r^2$ | SSE | $k_1 \times 10^{-3}$ | $r^2$ | SSE | $k_2 \times 10^{-3}$ | $r^2$ | SSE | $k_1 \times 10^{-3}$ | $r^2$ | SSE | $k_2 \times 10^{-3}$ | $r^2$ | SSE |
| $TiO_2$ | 187.2 | 0.93 | 77.97 | 16.1 | 0.97 | 0.24 | 2.5 | 0.71 | 0.08 | 13.1 | 0.99 | 7.42 | 0.6 | 0.93 | 83.05 |
| 1 mol% | 146.6 | 0.62 | 403.40 | 28.0 | 0.98 | 0.48 | 29.5 | 0.55 | 22.25 | 35.2 | 0.97 | 28.23 | 2.2 | 0.98 | 18.35 |
| 3 mol% | 97.6 | 0.90 | 31.63 | 11.2 | 1.00 | 0.01 | 1.7 | 0.92 | 0.01 | 12.1 | 0.99 | 2.09 | 0.9 | 0.97 | 9.39 |
| 5 mol% | 46.4 | 0.98 | 1.03 | 5.9 | 1.00 | 0.00 | 0.6 | 0.95 | 0.00 | 5.6 | 1.00 | 0.30 | 0.6 | 0.96 | 2.53 |
| 6.5 mol% | 24.2 | 1.00 | 0.09 | 4.9 | 0.99 | 0.01 | 0.8 | 0.92 | 0.00 | 4.4 | 0.98 | 0.32 | 0.8 | 0.94 | 1.06 |

**Table 3**
Optimization of tungsten-loaded synthesis.

| Sample | $k_1$ ($\times 10^{-3}$ min$^{-1}$) | $r^2$ | SSE |
|---|---|---|---|
| (A) Optimum tungsten loading | | | |
| 0-w-450-2 | 16.1 | 0.97 | 0.24 |
| 0.3-w-450-2 | 14.0 | 0.99 | 0.05 |
| 0.6-w-450-2 | 16.6 | 0.99 | 0.09 |
| 1-w-450-2 | 28.0 | 0.98 | 0.48 |
| 1.5-w-450-2 | 25.6 | 0.98 | 0.22 |
| 2-w-450-2 | 19.8 | 0.99 | 0.04 |
| 3-w-450-2 | 11.2 | 0.99 | 0.01 |
| 4-w-450-2 | 5.8 | 1.00 | 0.00 |
| 5-w-450-2 | 5.9 | 0.99 | 0.00 |
| 6.5-w-450-2 | 4.9 | 0.99 | 0.01 |
| 8-w-450-2 | 4.4 | 0.99 | 0.00 |
| 10-w-450-2 | 3.5 | 0.98 | 0.00 |
| 12-w-450-2 | 2.7 | 0.97 | 0.01 |
| 100-w-450-2 | 1.2 | 0.98 | 0.00 |
| (B) Optimum calcinations temperature | | | |
| 0-w-450-2 | 16.1 | 0.97 | 0.24 |
| 0-w-550-2 | 10.3 | 0.99 | 0.01 |
| 0-w-650-2 | 3.5 | 0.99 | 0.00 |
| 0-w-750-2 | 2.7 | 0.99 | 0.00 |
| 0-w-850-2 | 1.7 | 0.99 | 0.00 |
| 1-w-450-2 | 28.0 | 0.98 | 0.48 |
| 1-w-550-2 | 28.0 | 0.99 | 0.17 |
| 1-w-650-2 | 22.6 | 0.99 | 0.08 |
| 1-w-750-2 | 4.8 | 0.98 | 0.01 |
| 1-w-850-2 | 4.4 | 0.99 | 0.00 |
| (C) Optimum calcinations duration | | | |
| 1-w-450-0.5 | 18.0 | 0.97 | 0.23 |
| 1-w-450-1 | 20.0 | 0.98 | 0.15 |
| 1-w-450-2 | 28.0 | 0.98 | 0.49 |
| 1-w-450-4 | 18.4 | 0.98 | 0.14 |

degradation of 1,4-dichorobenzene using $WO_3$-loaded $TiO_2$ photocatalysts [40]. In a study on photocatalytic degradation and mineralization of formic acid, oxalic acid, 4-chlorophenol and manuron by $TiO_2$, oxalic and formic acid mineralizations have been reported to follow zeroth order kinetics without the formation of intermediates, while the degradation of 4-chlorophenol and manuron on the other hand follow first order kinetics [41].

### 3.4. Optimization of preparation procedure

The procedure of preparation was further optimized to achieve higher photocatalysis. The parameters optimized were tungsten loading, calcination temperatures and calcination duration and the results are summarized in Table 3.The amount of tungsten loaded onto $TiO_2$ plays an important role in its photocatalytic activity. Within the values ranging from 0 to 12 mol% $WO_3$, $TiO_2$ loaded with small amount of tungsten (<3 mol% $WO_3$), was active as a photocatalyst, while the one loaded with higher tungsten was active as an adsorbent. As a benchmark, the rate constant for unmodified $TiO_2$ was $16.1 \times 10^{-3}$ min$^{-1}$. The enhancement of photocatalytic activity ($k_1 = (16.5–28.0) \times 10^{-3}$ min$^{-1}$) appeared to occur at 0.6–2 mol% $WO_3$ loading range. At higher than 2 mol%, the photocatalytic activity decreased to $11.2 \times 10^{-3}$ min$^{-1}$ or lower. At lower than 0.6 mol% $WO_3$, the photocatalytic activity remained around $(14–16) \times 10^{-3}$ min$^{-1}$. At 1 mol% $WO_3$, the rate constant of $28.0 \times 10^{-3}$ min$^{-1}$, was approximately twice the rate constant of unmodified $TiO_2$. The lower rate contant at 2 mol% and beyond suggests the threshold level within the range of 1–2 mol% tungsten loading for optimum photocatalysis. The maximum improvement of MB degradation by flame-made $WO_3/TiO_2$ have been reportedly achieved at 3.6 mol% [33], while only 40–50% enhancement is observed when 3 mol% $WO_3/TiO_2$ is tested against MB [40]. When the surface of $TiO_2$ is covered with monolayer thickness theoretically at 3.2 mol% $WO_3$, the degradation of aqueous dichlorobenzene is enhanced by 2.5-fold, and benzene and 2-propanol degradation in the gas phase enhanced by 3.6- and 5.9-fold, respectively [40].

The optimum tungsten loading for MB degradation appears to be very much affected by preparation method. For example, $WO_x$–$TiO_2$ prepared using sol–gel method has the highest activity for degradation of MB under visible lamp at 3% $WO_3$ [39]. In addition, XPS analyses of 3 mol% $WO_3/TiO_2$ loading shows the existence of $W^{6+}$, $W^{5+}$, and $W^{4+}$ where the first two are predominant. It is suggested that $W^{4+}$ can substitute $Ti^{4+}$ due to the similarity in ionic radius, forming the non-stoichiometric solid solution $W_xTi_{1-x}O_2$. Optical absorption measurement reveals that doping with tungsten shifts the absorption spectrum to the visible region, though no clear absorption edge is observed. In another study, the $WO_x$–$TiO_2$ prepared by sol mixing method shows the optimum tungsten loading at 1 mol% [42]. In contradiction to that reported by Li et al. [39], XPS analysis of 1 mol% $WO_3/TiO_2$ shows the existence of $W^{4+}$, $W^{5+}$, and $W^{6+}$, but the first two are predominant. The similarity is however found in that the absorption spectrum of W-doped $TiO_2$ is found shifted to the visible light, and the photocatalytic activity of W-doped $TiO_2$ at 1 mol% $WO_3$ is superior to N-doped and C-doped $TiO_2$ [42].

Another factor which plays important role in the photocatalytic activity is the calcination temperature. In impregnation method upon heat treatment, the metal salt AMT will be transformed into the respective oxide, $WO_3$. The metastable anatase phase which is the active phase undergoes transformation into inactive rutile. Therefore, determination of optimum calcinations temperature is necessary. Table 3 summarizes the effect of calcinations temperatures on the photocatalytic activity of $TiO_2$ loaded with 1 mol% $WO_3$. The photocatalytic activity remained high at 550 °C, slightly decreased at 650 °C and significantly reduced at 750 and 850 °C. In comparison, the photocatalytic activity of unmodified $TiO_2$ already decreased when calcined at 550 °C and significantly reduced at 650 °C or higher. Hence, tungsten loading increased the stability of $TiO_2$ photocatalytic activity. Tungsten loading stabilizes the anatase phase from being transformed into rutile resulting in high photocatalytic activity maintained. The optimum calcinations length was found at 2 h, and calcinations at lower or higher than this, resulted in lower photocatalytic activity. The lower activity at too short calcination length may be due to incomplete transformation of AMT into $WO_3$, and at longer than 2 h due to high degree of aggregation.

### 3.5. Effect of UV filter

The metal halide clear lamp 4000 K used in this experiment emits both near UV and visible spectrum from 380 to 760 nm. Although the near UV spectrum covers only a small portion as compared to the visible spectrum, it is necessary to check the photocatalytic activity of the photocatalyst without the UV portion to have better understanding of its effect on the photocatalytic activity. A solution of sodium nitrite was used to remove the UV portion of the lamp [43]. As a control, water filter was used to simulate the photocatalytic activity under UV–visible light. The photocatalytic activity of unmodified $TiO_2$ and 1-w-450-2 with and without UV filter is shown in Fig. 7. The photocatalytic activities of both samples were significantly reduced when the UV filter was used. In the presence of water filter, the photocatalytic activity of unmodified $TiO_2$ and 1-w-450-2 were only slightly decreased as compared to those without any filter (data not shown). However, 1-w-450-2 had 2-fold higher photocatalytic activity than unmodified one and that the reductions in photocatalytic activities in both samples were proportional. This was due to the reduced light intensity reaching the suspension since part of it was deflected by the water filter. This result may also confirm the suggestion that MB decolourization through photosensitization mechanism is negligible [44]. The DRUV-Vis. measurement (data not shown) suggested

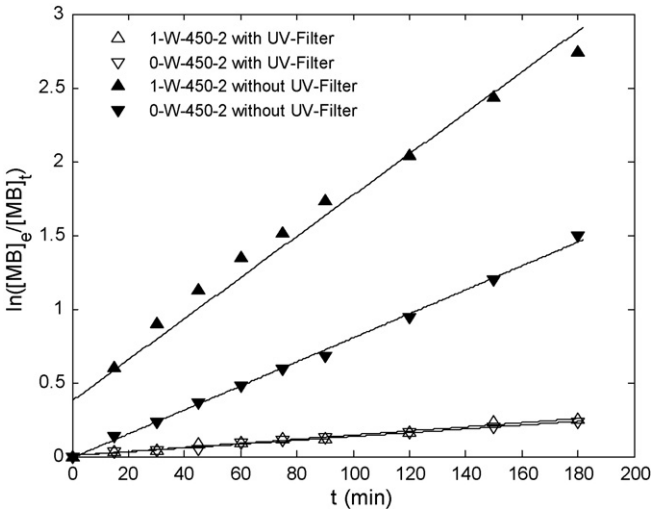


**Fig. 7.** The photocatalytic activity of pure $TiO_2$ and 1 mol% tungsten-loaded $TiO_2$ with and without UV filter.

that no shifting in the optical absorption of modified $TiO_2$ occurred [31]. Hence, our study showed that both photocatalysts were UV light activated, and the enhancement in photocatalytic activities were not due to the extension of photoresponse to the visible light spectrum as has been reported by other researchers [39,42]. Nevertheless, the photocatalytic activity of the photocatalyst under UV-visible light against MB is significantly improved with $WO_3$ doping as compared to unmodified $TiO_2$. Similar observation has also been reported where the photocatalytic activity of W-doped $TiO_2$ is better than bare $TiO_2$ for $\lambda = 365$, $\lambda > 420$, and $\lambda = 460$ nm which are all near UV and visible spectrum [42].

The enhanced photocatalytic activity of tungsten-loaded $TiO_2$ has been reported due to the enhanced adsorption and charge separation [33,38,40]. The photogenerated electrons can be trapped by $W^{6+}$ to form $W^{5+}$, while at the same time the presence of oxygen can re-oxidize $W^{5+}$ to $W^{6+}$ [33]. This may reduce the electron–hole pair recombination losses. The recombination losses have also been reportedly successfully reduced in the photoanode for solar energy conversion devices, combining $TiO_2$ and $WO_3$ films, in a two-layer arrangement [45,46]. In our study, tungsten-loaded $TiO_2$ had shown dual functions – as an adsorbent and a photocatalyst, depending on the tungsten loading. Decolourization of MB by tungsten-loaded $TiO_2$ can be achieved via adsorption and photocatalysis. At higher tungsten loadings, decolourization of MB via adsorption is more pronounced. On the other hand, decolourization via photocatalysis is more effective at lower tungsten loading. It is highly likely that the presence of tungsten on the surface of $TiO_2$ has significantly changed the surface polarity of $TiO_2$ as observed in the decreasing PZC value [31] and higher adsorption of MB.

## 4. Conclusions

Tungsten-loaded $TiO_2$ has been successfully prepared and optimized. The photocatalyst had both high photocatalytic activity and adsorption affinity towards MB. The adsorption ability of the photocatalyst was increased with increasing tungsten loadings up to 6.5 mol% $WO_3$. Adsorption isotherm study showed that the adsorption followed Langmuir model with maximum adsorption capacity of $95.9 \times 10^{-3}$ mmol $g^{-1}$, which was 8-fold higher than the reported value for unmodified $TiO_2$. Kinetic studies suggested that the photocatalytic degradation of MB followed first order kinetics. The optimum synthesis condition was found at 1 mol% tungsten loading and calcination at 450 °C for 2 h. The enhanced photocatalytic activity of tungsten-loaded $TiO_2$ was not due to the extension of the photoresponse into the visible region but possibly due to the increased adsorption and better charges separation. Our study has demonstrated that the tungsten-loaded $TiO_2$ has dual functions – as an adsorbent and photocatalyst, depending on the tungsten loading.

## Acknowledgements

The authors would like to thank Universiti Teknologi Petronas for providing the research facilities and scholarship to Saepurahman. The Short Internal Research Fund (STIRF) Grant no. 10/06.07 that funded this project is highly appreciated. Many thanks to Mr Edwar Yazid from the Department of Mechanical Engineering and Mr Esa Prakasa from the Department of Electrical and Electronics Engineering, Universiti Teknologi Petronas, for some discussions on MATLAB.

## References

[1] V.N. Parmon, Photocatalysis as a phenomenon: aspects of terminology, Catal. Today 39 (1997) 137–144.
[2] Titanium, http://en.wikipedia.org/wiki/Titanium (accessed December 24, 2009).
[3] I.K. Konstantinou, T.A. Albanis, $TiO_2$-assisted photocatalytic degradation of azo dyes in aqueous solution: kinetic and mechanistic investigations: a review, Appl. Catal. B 49 (2004) 1–14.
[4] Z. Wang, W. Cai, X. Hong, X. Zhao, F. Xu, C. Cai, Photocatalytic degradation of phenol in aqueous nitrogen-doped $TiO_2$ suspensions with various light sources, Appl. Catal. B 57 (2005) 223–231.
[5] M.R. Hoffmann, S.T. Martin, W. Choi, D.W. Bahnemann, Environmental applications of semiconductor photocatalysis, Chem. Rev. 95 (1995) 69–96.
[6] N.S. Lewis, Light work with water, Nature 414 (2001) 589–590.
[7] Y. Bessekhouad, D. Robert, J.V. Weber, N. Chaoui, Effect of alkaline-doped $TiO_2$ on photocatalytic efficiency, J. Photochem. Photobiol. A 167 (2004) 49–57.
[8] N. Venkatachalam, M. Palanichamy, B. Arabindoo, V. Murugesan, Alkaline earth metal doped nanoporous $TiO_2$ for enhanced photocatalytic mineralisation of bisphenol-A, Catal. Commun. 8 (2007) 1088–1093.
[9] Y. Li, S. Peng, F. Jiang, G. Lu, S. Li, Effect of doping $TiO_2$ with alkaline-earth metal ions on its photocatalytic activity, J. Serb. Chem. Soc. 72 (2007) 393–402.
[10] J. Chen, M. Yao, X. Wang, Investigation of transition metal ion doping behaviors on $TiO_2$ nanoparticles, J. Nanopart. Res. 10 (2008) 163–171.
[11] V. Brezová, A. Blažková, L. Karpinský, J. Grošková, B. Havlínová, V. Jorík, M. Ceppan, Phenol decomposition using $M^{n+}/TiO_2$ photocatalysts supported by the sol–gel technique on glass fibres, J. Photochem. Photobiol. A 109 (1997) 177–183.
[12] S.M. Karvinen, The effects of trace element doping on the optical properties and photocatalytic activity of nanostructured titanium dioxide, Ind. Eng. Chem. Res. 42 (2003) 1035–1043.
[13] A. Di Paola, Transition metal doped $TiO_2$: physical properties and photocatalytic behaviour, Int. J. Photoenergy 3 (2001) 171–176.
[14] A.W. Xu, Y. Gao, H.Q. Liu, The preparation, characterization, and their photocatalytic activities of rare-earth-doped $TiO_2$ nanoparticles, J. Catal. 207 (2002) 151–157.
[15] Y. Wang, H. Cheng, L. Zhang, Y. Hao, J. Ma, B. Xu, W. Li, The preparation, characterization, photoelectrochemical and photocatalytic properties of lanthanide metal-ion-doped $TiO_2$ nanoparticles, J. Mol. Catal. A: Chem. 151 (2000) 205–216.
[16] J.C. Colmenares, M.A. Aramendía, A. Marinas, J.M. Marinas, F.J. Urbano, Synthesis, characterization and photocatalytic activity of different metal-doped titania systems, Appl. Catal. A 306 (2006) 120–127.
[17] A. Di Paola, E. Garciïa-López, S. Ikeda, G. Marci, B. Ohtani, L. Palmisano, Photocatalytic degradation of organic compounds in aqueous systems by transition metal doped polycrystalline $TiO_2$, Catal. Today 75 (2002) 87–93.
[18] A. Di Paola, E. García-López, G. Marcì, C. Martín, L. Palmisano, V. Rives, A. Maria Venezia, Surface characterisation of metal ions loaded $TiO_2$ photocatalysts: structure–activity relationship, Appl. Catal. B 48 (2004) 223–233.
[19] A. Di Paola, G. Marci, L. Palmisano, M. Schiavello, K. Uosaki, S. Ikeda, B. Ohtani, Preparation of polycrystalline $TiO_2$ photocatalysts impregnated with various transition metal ions: characterization and photocatalytic activity for the degradation of 4-nitrophenol, J. Phys. Chem. B 106 (2002) 637–645.
[20] Y. Anjaneyulu, N. Sreedhara Chary, D. Samuel Suman Raj, Decolourization of industrial effluents–available methods and emerging technologies–a review, Rev. Environ. Sci. Biotechnol. 4 (2005) 245–273.
[21] K. Hunger, Industrial Dyes: Chemistry, Properties and Applications, Wiley–VCH, Heidelberg, 2003.
[22] S. Bekkouche, M. Bouhelassa, N.H. Salah, F.Z. Meghlaoui, Study of adsorption of phenol on titanium oxide ($TiO_2$), Desalination 166 (2004) 355–362.
[23] M.A. Abdullah, L. Chiang, M. Nadeem, Comparative evaluation of adsorption kinetics and isotherms of a natural product removal by Amberlite polymeric adsorbents, Chem. Eng. J. 146 (2009) 370–376.

[24] A. Bhattacharyya, S. Kawi, M.B. Ray, Photocatalytic degradation of orange II by $TiO_2$ catalysts supported on adsorbents, Catal. Today 98 (2004) 431–439.
[25] C. Zhu, L. Wang, L. Kong, X. Yang, L. Wang, S. Zheng, F. Chen, F. MaiZhi, H. Zong, Photocatalytic degradation of AZO dyes by supported $TiO_2$ + UV in aqueous solution, Chemosphere 41 (2000) 303–309.
[26] F. Li, S. Suna, Y. Jiang, M. Xia, M. Sun, B. Xue, Photodegradation of an azo dye using immobilized nanoparticles of $TiO_2$ supported by natural porous mineral, J. Hazard. Mater. 152 (2008) 1037–1044.
[27] M. Huang, C. Xu, Z. Wu, Y. Huang, J. Lin, J. Wu, Photocatalytic discolorization of methyl orange solution by Pt modified $TiO_2$ loaded on natural zeolite, Dyes Pigments 77 (2008) 327–334.
[28] A. Neren Okte, O. Yılmaz, Photodecolorization of methyl orange by yttrium incorporated $TiO_2$ supported ZSM-5, Appl. Catal. B: Environ. 85 (2008) 92–102.
[29] H. Lachheb, E. Puzenat, A. Houas, M. Ksibi, E. Elaloui, C. Guillard, J.M. Herrmann, Photocatalytic degradation of various types of dyes (Alizarin S, Crocein Orange G, Methyl Red, Congo Red, Methylene Blue) in water by UV-irradiated titania, Appl. Catal. B 39 (2002) 75–90.
[30] T. Sauer, G. Cesconeto Neto, H.J. José, R. Moreira, Kinetics of photocatalytic degradation of reactive dyes in a $TiO_2$ slurry reactor, J. Photochem. Photobiol. A 149 (2002) 147–154.
[31] Saepurahman, M.A. Abdullah, F.K. Chong, Preparation and characterization of tungsten-loaded titanium dioxide photocatalyst for enhanced dye degradation, J. Hazard. Mater., doi:10.1016/j.jhazmat.2009.11.050.
[32] C.H. Liang, F.B. Li, C.S. Liu, J.L. Lü, X.G. Wang, The enhancement of adsorption and photocatalytic activity of rare earth ions doped $TiO_2$ for the degradation of Orange I, Dyes Pigments 76 (2008) 477–484.
[33] K.K. Akurati, A. Vital, J.-P. Dellemann, K. Michalow, T. Graule, D. Ferri, A. Baiker, Flame-made $WO_3/TiO_2$ nanoparticles: relation between surface acidity, structure and photocatalytic activity, Appl. Catal. B 79 (2008) 53–62.
[34] N. Couselo, F.S. GarciaEinschlag, R.J. Candal, M. Jobbagy, Tungsten-doped $TiO_2$ vs. pure $TiO_2$ photocatalysts: effects on photobleaching kinetics and mechanism, J. Phys. Chem. C 112 (2008) 1094–1100.
[35] V. Iliev, D. Tomova, L. Bilyarska, A. Eliyas, L. Petrov, Photocatalytic properties of $TiO_2$ modified with platinum and silver nanoparticles in the degradation of oxalic acid in aqueous solution, Appl. Catal. B 63 (2006) 266–271.
[36] V. Iliev, D. Tomova, R. Todorovska, D. Oliver, L. Petrov, D. Todorovsky, M. Uzunova-Bujnova, Photocatalytic properties of $TiO_2$ modified with gold nanoparticles in the degradation of oxalic acid in aqueous solution, Appl. Catal. A 313 (2006) 115–121.
[37] V. Iliev, D. Tomova, L. Bilyarska, G. Tyuliev, Influence of the size of gold nanoparticles deposited on $TiO_2$ upon the photocatalytic destruction of oxalic acid, J. Mol. Catal. A: Chem. 263 (2007) 32–38.
[38] C. Martín, G. Solana, V. Rives, G. Marcì, L. Palmisano, A. Sclafani, Physicochemical properties of $WO_3/TiO_2$ systems employed for 4-nitrophenol photodegradation in aqueous medium, Catal. Lett. 49 (1997) 235–243.
[39] X.Z. Li, F.B. Li, C.L. Yang, W.K. Ge, Photocatalytic activity of $WO_x$–$TiO_2$ under visible light irradiation, J. Photochem. Photobiol. A 141 (2001) 209–217.
[40] Y. Tae Kwon, K. Yong Song, W. In Lee, G. Jin Choi, Y. Rag Do, Photocatalytic behavior of $WO_3$-loaded $TiO_2$ in an oxidation reaction, J. Catal. 191 (2000) 192–199.
[41] J. Krýsa, G. Waldner, H. Mešťánková, J. Jirkovský, G. Grabner, Photocatalytic degradation of model organic pollutants on an immobilized particulate $TiO_2$ layer: roles of adsorption processes and mechanistic complexity, Appl. Catal. B 64 (2006) 290–301.
[42] H. Song, H. Jiang, X. Liu, G. Meng, Efficient degradation of organic pollutant with $WO_x$ modified nano $TiO_2$ under visible irradiation, J. Photochem. Photobiol. A 181 (2006) 421–428.
[43] D. Chatterjee, V.R. Patnam, A. Sikdar, P. Joshi, R. Misra, N.N. Rao, Kinetics of the decoloration of reactive dyes over visible light-irradiated $TiO_2$ semiconductor photocatalyst, J. Hazard. Mater. 156 (2007) 435–441.
[44] K. Tennakone, S. Punchihewa, S. Wickremanayaka, R.U. Tantrigoda, Titanium dioxide catalysed photo-oxidation of methyl violet, J. Photochem. Photobiol. A 46 (1989) 247–252.
[45] S. Irina, H. Maria, Decrease of recombination losses in bicomponent $WO_3/TiO_2$ films photosensitized with cresyl violet and thionine, J. Electrochem. Soc. 145 (1998) 3981–3985.
[46] S. Irina, H. Maria, Bicomponent $WO_3/TiO_2$ films as photoelectrodes, J. Electrochem. Soc. 146 (1999) 243–249.